SOLUTION MINING RESEARCH INSTITUTE
105 Apple Valley Circle
Clarks Summit, PA 18411, USA

Telephone: +1 570-585-8092
Fax: +1 570-585-8091
www.solutionmining.org ◆ smri@solutionmining.org

Technical Conference Paper

Numerical Computations Of The Mechanical Behavior Of Cemented Casings Submitted To Large And Fast Pressure Variations

Benoit Brouard, Brouard Consulting, Paris, France
Pierre Bérest, Ecole Polytechnique, Palaiseau, France
Claude Caligaris, Gaz de France, Clichy, France
Attilio Frangi, Politecnico di Milano, Milano, Italy
Grégoire Hévin, Gaz de France, Clichy, France
Thierry Pichery, Gaz de France, France

Fall 2006 Conference
1-4 October
Rapid City, South Dakota, USA

Solution Mining Research Institute, Fall 2006 Technical Meeting
Rapid City, USA, October 1-4, 2006

NUMERICAL COMPUTATIONS OF THE MECHANICAL BEHAVIOR OF CEMENTED CASINGS SUBMITTED TO LARGE AND FAST PRESSURE VARIATIONS

B. Brouard[1], P. Bérest[2], C. Caligaris[3], A. Frangi[4], G. Hévin[3], T. Pichery[5]

[1] Brouard Consulting, Paris, France

[2] LMS, Ecole Polytechnique, Palaiseau, France

[3] Gaz de France, GDI, Clichy, France

[4] Politecnico di Milano, Milano, Italy

[5] Gaz de France, DEP, Saint Denis, France

ABSTRACT

The mechanical behavior of a salt cavern has been studied extensively for many years, but little is known about the behavior of cementations submitted to sharp pressure variations. This problem is of concern for the short-term integrity of hydrocarbon storage facilities and for the long-term integrity of abandoned caverns. Dedicated software has been developed to model fully the geometry of a well, taking into account various constitutive laws for the materials, and to compute the stress fields when the well is submitted to a complex loading history. Elasto-visco-plastic behaviors of cement and salt are taken into account. A pessimistic worst-case accident scenario is considered, and stresses are computed as a function of time to verify that no tensile stresses appear in the cement. A sensibility study is performed that takes uncertainties of material parameters into account.

Keywords: Cement evaluation, Computer modeling, Safety, Mechanical integrity

1. Introduction

In several countries, including France, underground gas storages architecture includes a production string and an annular space closed at the casing seat by a packer and filled with soft water (Figure 1). A small nitrogen column is set above the water column at the top of the annular space, and the nitrogen pressure is measured frequently. If, for any reason, a gas leak through the production string occurs, then the leaking gas is trapped in the annular space and detected by an increase in annular pressure at the wellhead.

Because the nitrogen+methane pressure at wellhead increases when the leak is perennial, it becomes important to assess whether the cement could be damaged when the annular pressure becomes high —particularly when it reaches the Maximum Allowable Wellhead Operating Pressure (MAWOP). The area of most concern is that near the packer, where a single cemented casing is present.

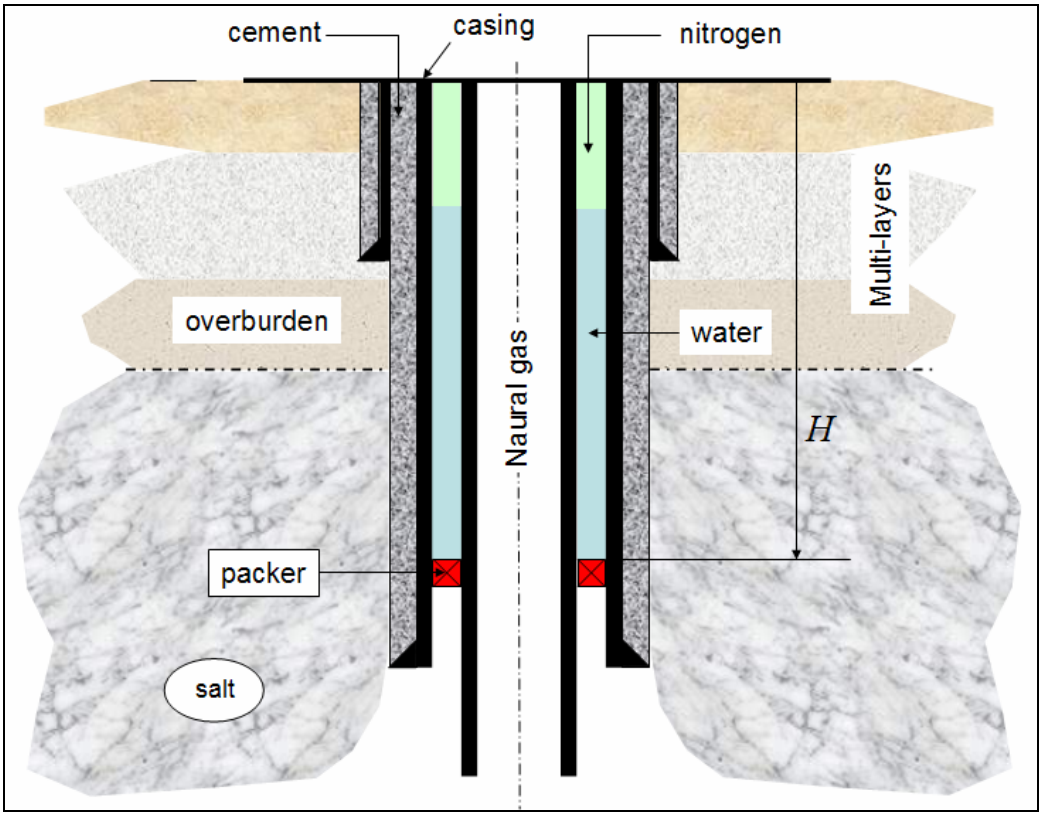

Figure 1 Typical well architecture for French natural-gas storages.

Finite element analyses were performed to simulate a worst-case scenario to determine whether tensile stresses could appear in the cement close to the packer. As the mechanical behavior of cement is not well known, a sensibility study was performed.

2. Study Strategy

To determine if the cement can be damaged, the following tasks were included in this study:

(1) full modeling of the well architecture;

(2) considerations of a worst-case scenario;

(3) accounting for a conservative criterion for cement damage;

(4) numerical analysis using finite elements computations; and

(5) a sensibility study for material parameters.

3. Modeling of Well Architecture

LOCAS is a semi-analytical, finite element code that provides 2D axisymmetric analysis (Brouard *et al.*, 2006). One part of *LOCAS* was developed to model well architecture and to perform analytical and finite elements computations regarding the mechanical behavior of a well. Analytical closed-form solutions were calculated to check the results of the finite element code. Using the embedded databases for the geometrical and mechanical characteristics of strings and sections, the software allows the user to draw a sketch of the well architecture (Figure 2); a close-up of the packer area is shown in Figure 3.

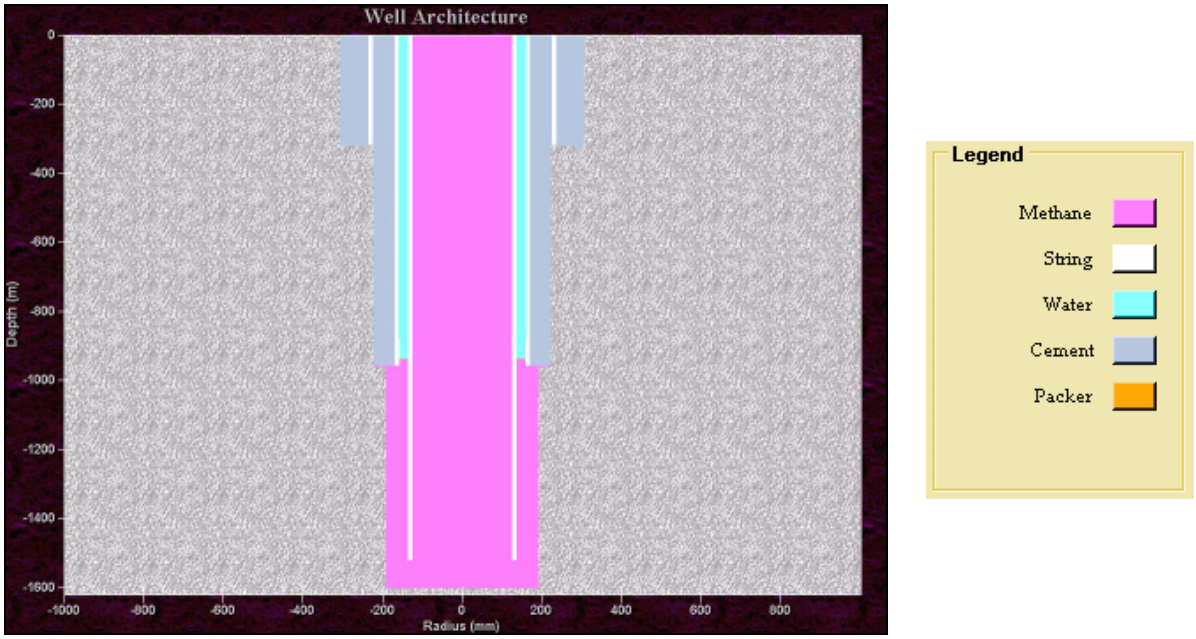

Figure 2 Example of a sketch of a well architecture. (The packer cannot be seen at this scale.)

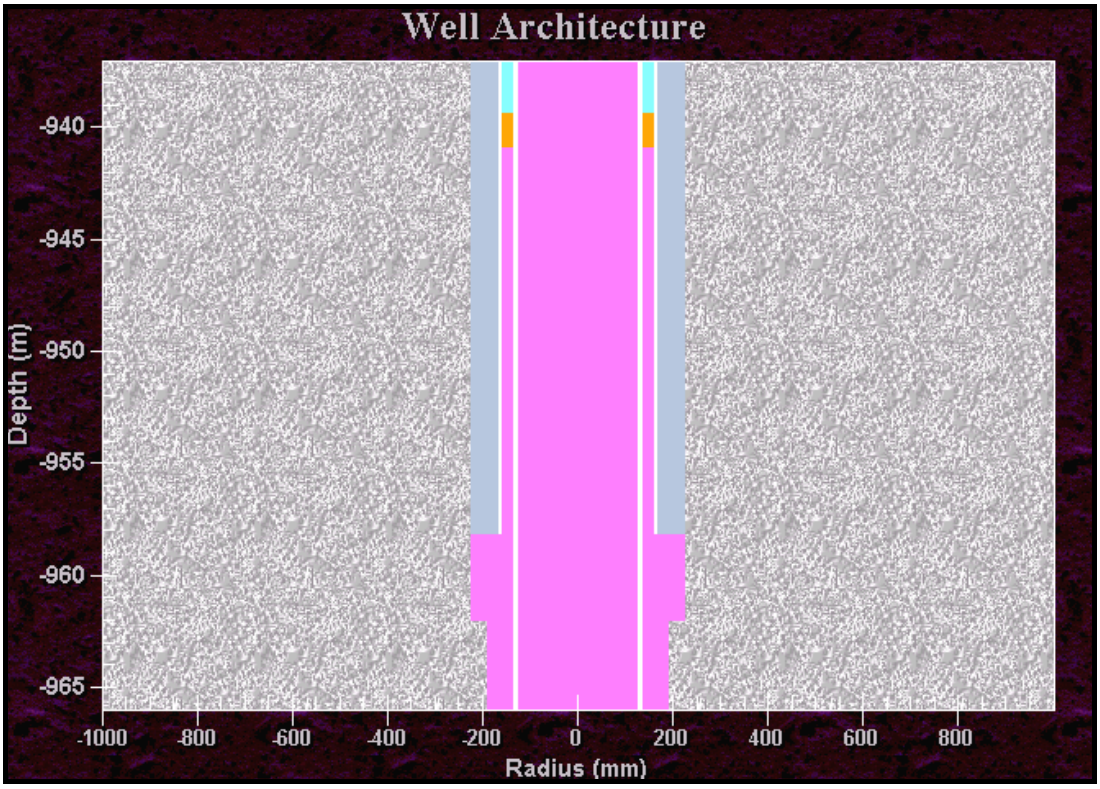

Figure 3 Well architecture in the vicinity of the packer.

4. Finite Element Modeling

Finite element modeling was used to determine stress field evolutions in the cement during a worst-case scenario.

4.1 Model Geometry and Boundary Conditions

Because well length is much greater than its width, full meshing of the well and rock mass would require huge meshes including millions of elements; it is much easier to consider thin well slices and to apply the relevant boundary conditions.

The model geometry used in the packer area is shown on Figure 4. (The correct scale and proportions are not maintained — e.g., areas of the string and cement are exaggerated to make them more visible in this sketch.) A slice a few meters thick is considered, as it has been proven that a 4-m thick slice is sufficient to avoid boundary effects. The boundary conditions are shown on Figure 5; there is no vertical displacement on the upper and bottom borders.

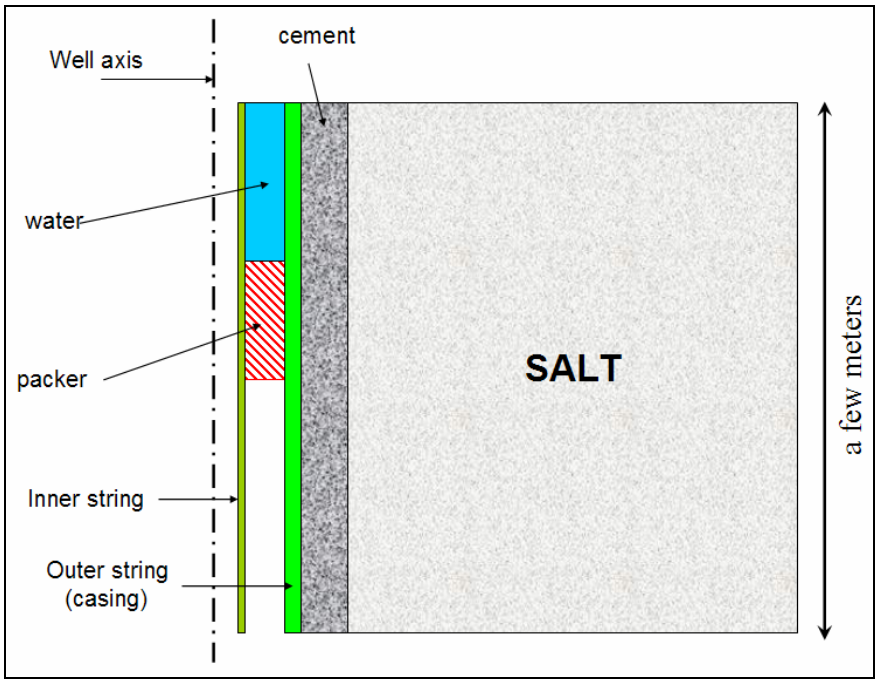

Figure 4 Packer area model.

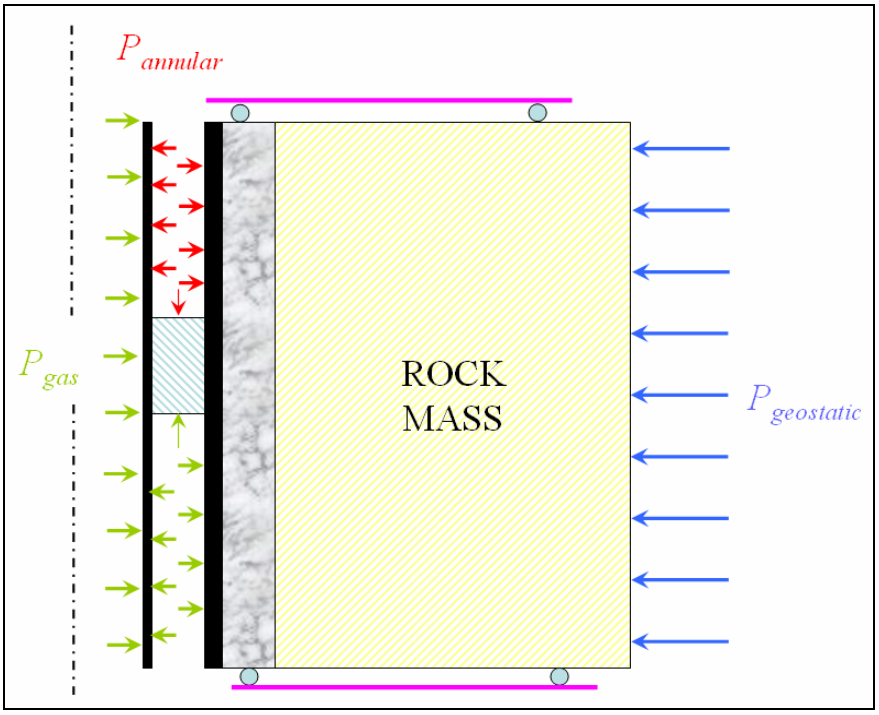

Figure 5 Boundary conditions.

4.2 Finite Element Model

LOCAS generates triangle elements; a mesh example is given on Figure 6.

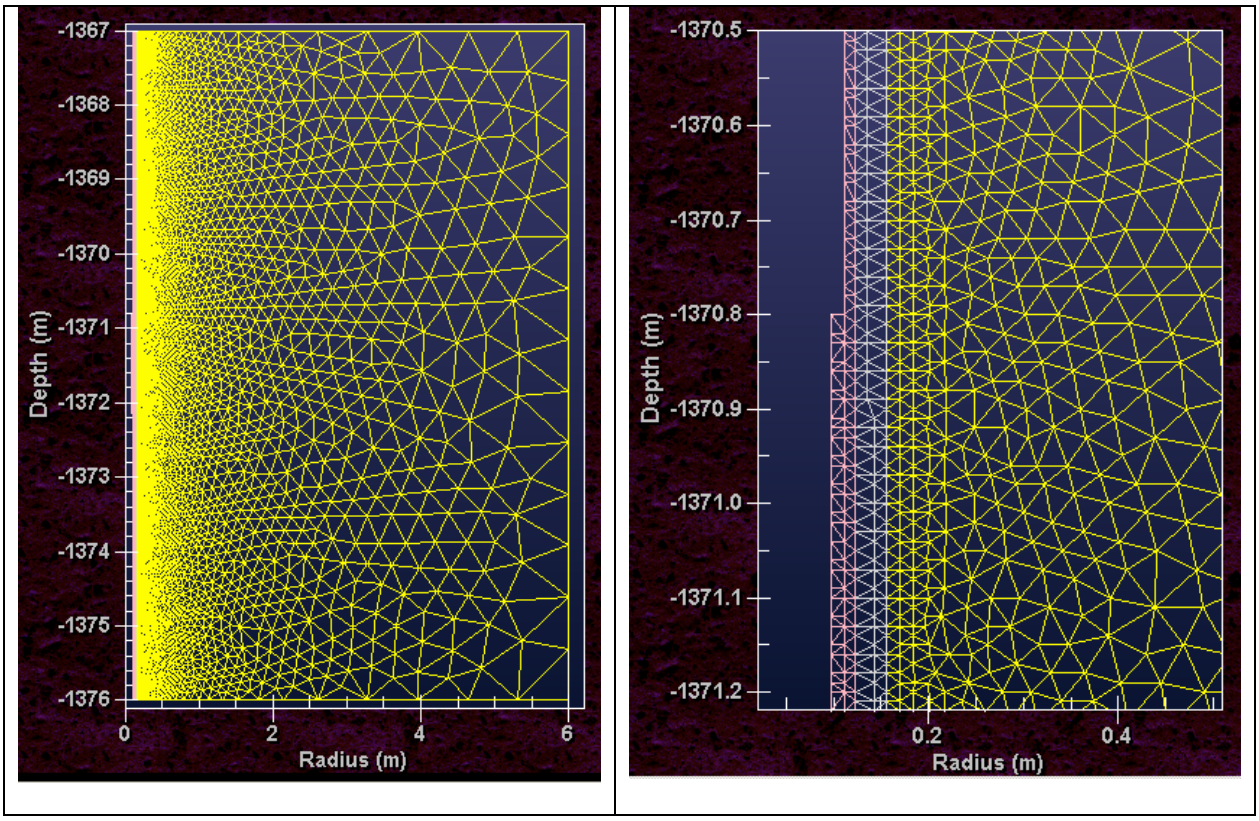

Figure 6 – Mesh example in packer area (close-up on the right).

5. Worst-Case Scenario

At the beginning of the study, it was expected that tensile stresses might appear in the cement when the pressure in the annular space is high and the gas pressure in the cavern is low. In that situation, there is a large pressure difference between the upper and lower sides of the packer, respectively submitted to annulus water pressure and gas cavern pressure.

- On the upper side, high pressure in the annular space can be achieved when gas has seeped from the cavern over a long period of time. If a methane leak appears, methane is trapped at the top of the annular space and mixes with nitrogen. However, when gas pressure at the wellhead reaches the Maximum Allowable Wellhead Operating Pressure (MAWOP), facility operators usually vent some gas. In the worst-case scenario, MAWOP is reached.
- On the lower side, cavern pressure can be low for several reasons — for example, at the end of a period of chilly weather. In the worst-case scenario, a blowout leading to a fast pressure drop was considered. [Such a scenario is considered often in Germany for gas-storage design studies, which focus on cavern behavior following a drastic pressure drop (Rokhar et al., 2004).]

Furthermore, the scenario is even more unfavorable when cavern pressure has been kept high for a long time (say, several months) before the fast pressure drop occurs. The evolution of production-string pressure, the wellhead annular pressure and the water pressure in the annular space during this worst-case scenario are shown on Figure 7, Figure 8 and Figure 9, respectively.

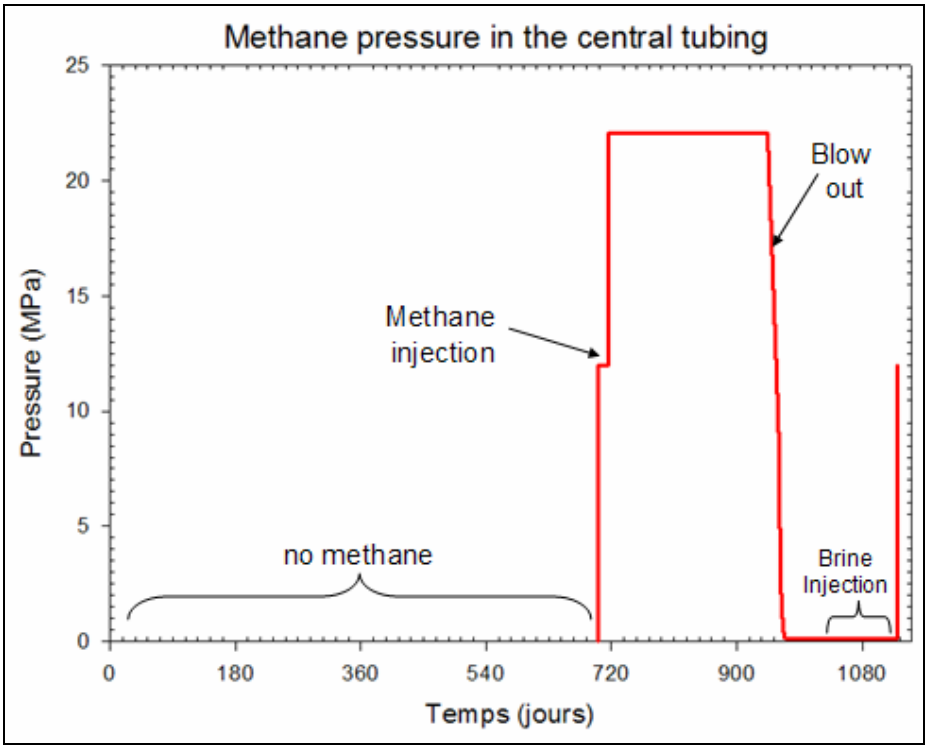

Figure 7 Methane pressure evolution in the production string.

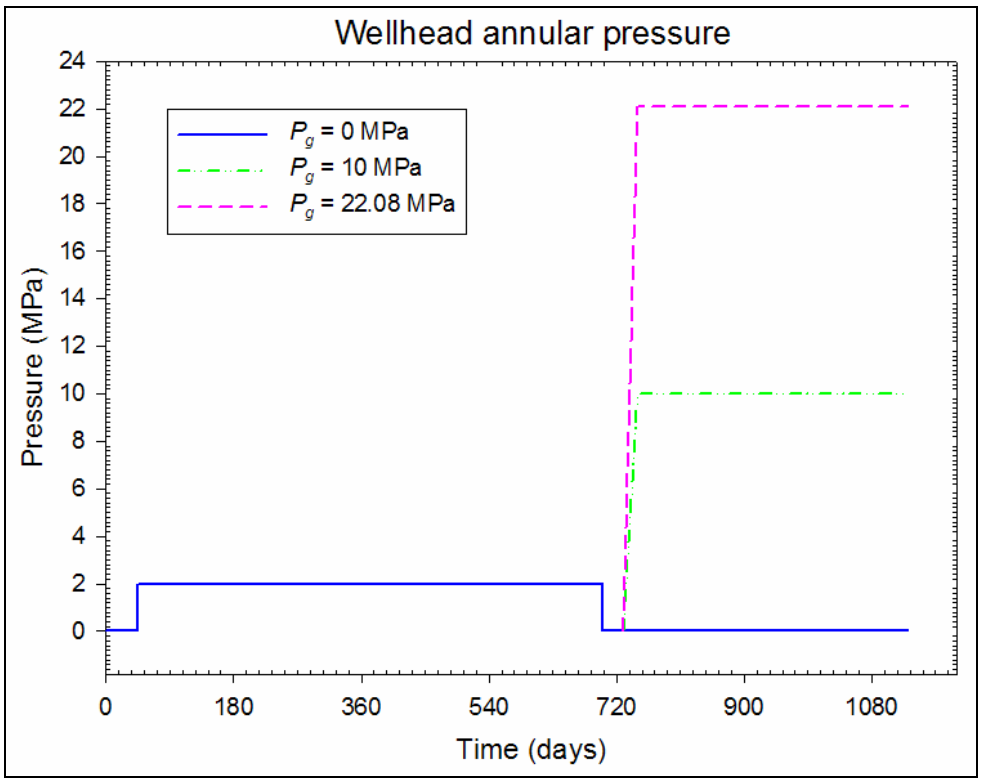

Figure 8 Evolution of wellhead annular pressure.

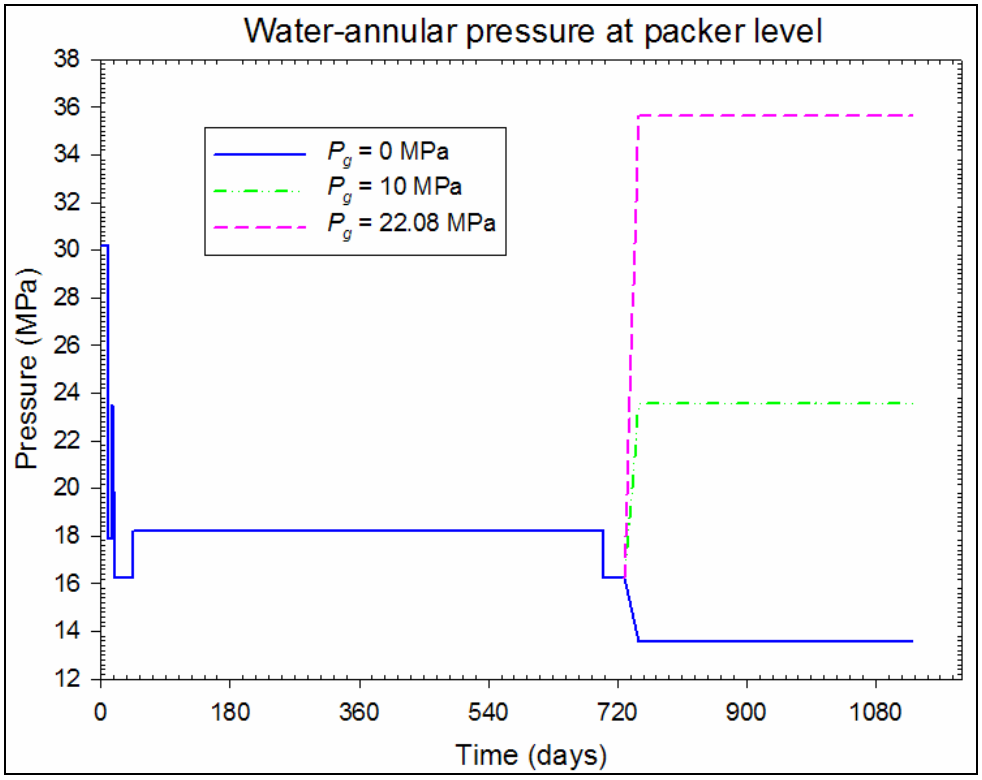

Figure 9 Evolution of water pressure in the annulus at packer level. (When a gas leak appears (day 730), two possibilities are considered: (1) the wellhead annular pressure quickly reaches the MAWOP ($P_g = 22.08$ MPa, in this example) and later is kept constant through gas withdrawals (magenta dashed line); or (2) the annular pressure reaches a certain threshold and the leak stops (dot-dashed green line). If there is no gas leak, the water pressure in the annulus at the packer level decreases when brine is replaced by soft water.)

The worst-case scenario is composed of the following phases:

- From day 0 (well drilling), The well is filled with mud.
- The upper casing is lowered.
- The upper casing is cemented.
- Drilling is carried out.
- The lower casing is lowered.
- The lower casing is cemented.
- Cavern leaching — The average cavern pressure is assumed to be 2 MPa above halmostatic pressure (i.e., the pressure resulting at depth from the weight of a saturated-brine column) due to head losses.
- Day 700 — End of leaching.
- The annular space is filled with soft water.
- The packer is set just above the seat of the last cemented casing. Some nitrogen is injected at the top of the annular space.
- From day 715, natural gas is injected into the cavern.
- The cavern is filled, and its pressure increases to the maximum pressure (22 MPa on Figure 7).
- Cavern pressure is kept high for a few months.
- On day 730,— a gas leak appears; the wellhead annular pressure increases more or less rapidly.
- From day 945, some gas is withdrawn on a regular basis from the annular space to keep the pressure constant and equal to MAWOP.
- Methane is withdrawn from the production string at a normal rate.
- A blowout takes place; then, cavern pressure decreases to atmospheric pressure over a week.
- Cavern pressure is low for several months; brine or water is injected into the cavern.
- Brine reaches the last casing seat on day 1130; halmostatic pressure is reached on day 1131.

Water pressure at packer depth (Figure 9 and Figure 10) is taken equal to geostatic pressure before drilling (No well yet exists.) and equals the pressure of a mud-filled column after drilling. It is assumed that the slurry (density 1.8) is injected after a few days. The mechanical behavior of the cement during grouting is not well known. In this study, it is assumed that annular pressure slowly decreases over 3 days to halmostatic pressure. The cavern leaching should start on day 45 and is over on day 700. Then, the annular space is filled with soft water, the packer is set just above the last cemented casing, and a nitrogen blanket is injected at the top of the annular space. When the gas leak appears on day 730, the methane is trapped at the wellhead and mixes with nitrogen, increasing wellhead pressure in the annular space. Several leaks rates were considered in this study; in an additional computation, it was assumed that leaks stop when the annular pressure reaches a certain threshold.

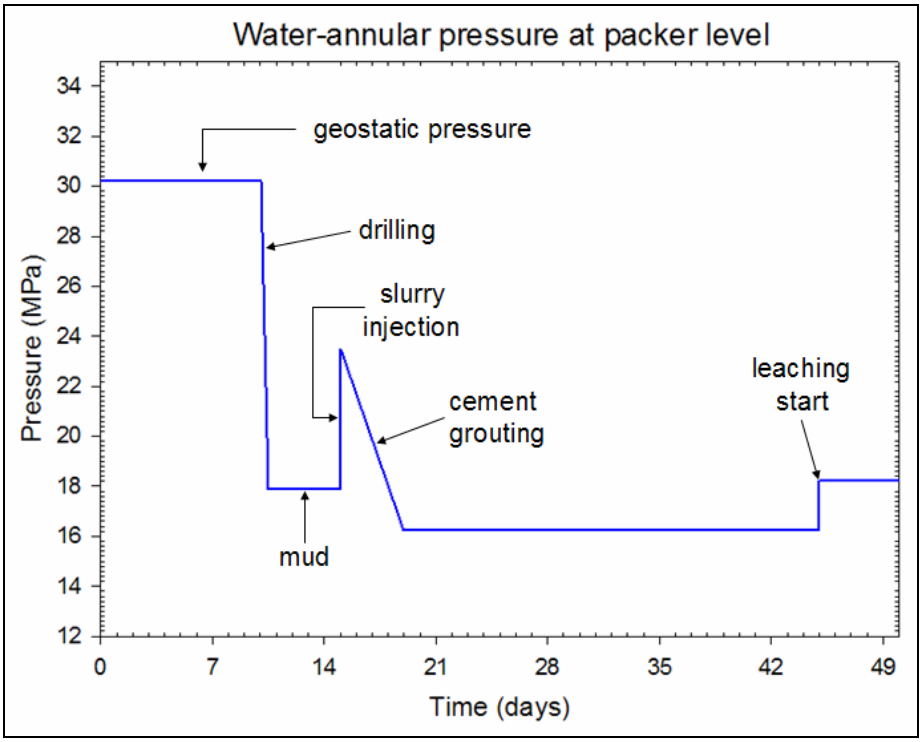

Figure 10 Water pressure evolution in the annular space during the first days after drilling.

6. Material Parameters

6.1 Salt Mechanical Behavior

Elastic Behavior — The following set of parameters for salt elasticity was used as a reference in the sensibility study:

$$E_{salt} = 25 \text{ GPa} \qquad \text{et} \qquad \nu_{salt} = 0.25$$

Viscoplastic Behavior — For underground storage in salt, French companies often use the Lemaitre-Menzel-Schreiner (L-M-S) law to model the transient viscoplastic behavior of salt, whose uniaxial formulation can be written:

$$\varepsilon^{vp} = \frac{\sigma^{\beta}}{K} t^{\alpha} \tag{1}$$

where ε^{vp} is the viscoplastic strain, σ is the (constant) applied load, and (α, β, K) are three independent parameters.

Gaz de France holds sets of maximum/minimum mechanical parameter values for each of its storage sites (see example in Table 1). There is no secondary creep in L-M-S law, but the law is convenient for short-term computations — especially cycling loads.

Table 1 Example of L-M-S minimum and maximum parameter sets for a French salt storage facility.

L-M-S Parameter	Minimum Set	Maximum Set
α	0.326	0.210
β	3.63	2.55
K (MPa)	1.115	1.075

6.2 The Mechanical Behavior of Cement

There currently is a lack of knowledge concerning the mechanical behavior of cement used in underground storage. Because cement properties depend on its components as well as on grouting conditions, it is likely that a relatively large range of elastic parameters must be expected. Szary et al. (2004) have performed laboratory tests to determine the mechanical behavior of cement used for gas storage in salt caverns in Germany.

Elastic Behavior — The following set of elastic parameters, reported by Szary et al. (2004) were used as a reference set:

$$E_{cem} = 12 \text{ GPa} \qquad \text{et} \qquad \nu_{\text{cem}} = 0.25$$

Viscoplastic Behavior — Szary et al. (2004) selected a viscoplastic behavior for cement (Figure 11). We back-calculated parameters for the Munson-Dawson law from the results of their creep tests.

The Munson-Dawson (M-D) creep law (Munson, 1997) originally was developed in the context of radioactive waste disposal, and there are more than a dozen parameters for this model, which encompasses a large domain of stresses and temperatures. A simplified version of the M-D model is considered here:

$$\dot{\varepsilon}^{vp} = F \cdot \dot{\varepsilon}^{s} \quad \text{where} \quad \dot{\varepsilon}^{s} = A_1 \, exp\left(-\frac{Q}{RT}\right)\sigma^{n} \tag{2}$$

where $\dot{\varepsilon}^{vp}$ is the transient-viscoplastic strain rate, $\dot{\varepsilon}^{s}$ is the stationary-viscoplastic strain rate, σ is the effective stress, and F is a function of an internal variable ζ :

$$\dot{\zeta} = (F-1)\cdot\dot{\varepsilon}^{s} \tag{3}$$

$$F = \begin{cases} e^{\Delta\left(1-\zeta/\varepsilon_t^*\right)^2} & \text{for } \zeta \le \varepsilon_t^* \\ 1 & \text{for } \zeta = \varepsilon_t^* \\ e^{-\delta\left(1-\zeta/\varepsilon_t^*\right)^2} & \text{for } \zeta \ge \varepsilon_t^* \end{cases} \tag{4}$$

$$\varepsilon_t^* = K_0 e^{-cT}\sigma^{m} \quad \left(e^{-cT} \approx 1\right) \tag{5}$$

$$\Delta = \alpha_w + \beta_w Log_{10}\frac{\sigma}{\mu} \tag{6}$$

where T is the absolute temperature, and μ is a constant. There are 9 independent material parameters in the considered version of the M-D law:

$$A_1,\ Q/R,\ n,\ m,\ \alpha_w,\ \beta_w,\ \delta,\ K_o,\ c.$$

Temperature dependency was not taken into account in this study ($c = 0$).

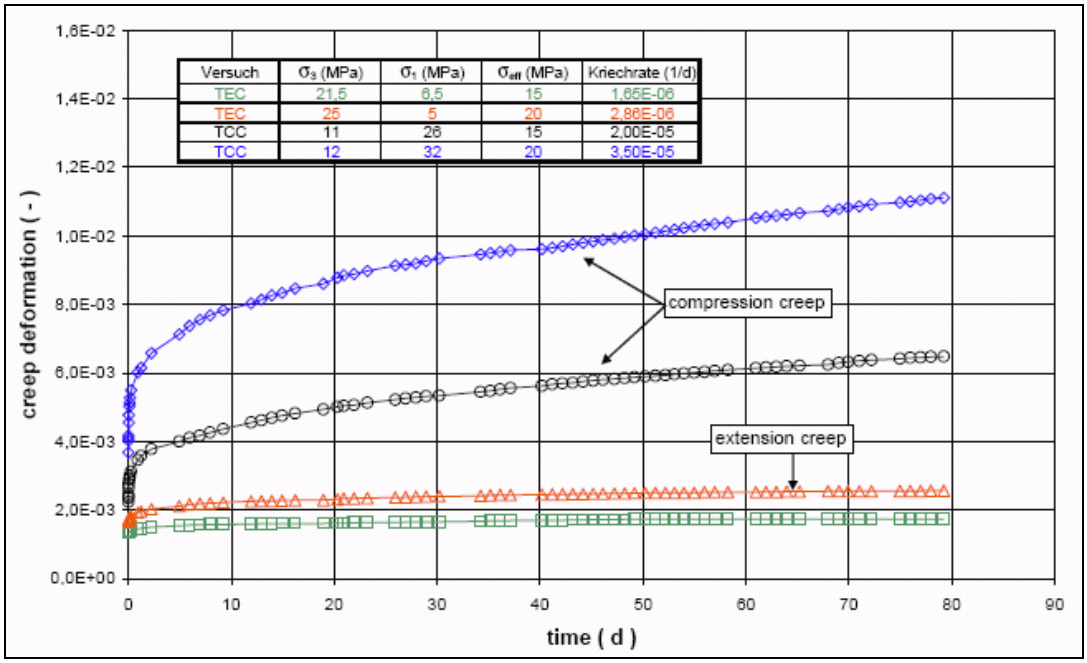

Figure 11 Cement creep behavior under triaxial conditions, both in compression and in extension (after Szary et al., 2004).

From the Szary et al. (2004) data, a reference set for the M-D law has been determined:

$$A_1 \exp\left(-\frac{Q}{RT}\right) = 1.03 \cdot 10^{-7} \ /\text{day-MPa}^{1.95} \qquad n = 1.95$$

$$K_0 = 1.59 \cdot 10^{-5} \ /\text{MPa}^2 \qquad m = 2$$

$$\alpha_w \approx 24.42 \qquad \beta_w \approx 4.16 \qquad \delta \approx 12$$

6.2 The Mechanical Behavior of Clay

A modified Cam-Clay law also was implemented in *LOCAS* in order to take into account the case of cement being in contact with clayey layers. This option was not used in the computations presented in this paper.

6.3 Cement Failure Criterion

A conservative no-tension criterion was selected for the cement.

7. Sensibility Study

The relative influence of several parameters on the evolution of stress in cement is difficult to forecast; this is why it is relevant to perform a sensibility study to take into account uncertainties regarding material parameters, especially cement properties. Considered parameters and their domain of variations are shown in Table 2.

Table 2 Parameters for the mechanical behavior of salt and cement in the computations.

Material	Behavior	Parameter	Unit	Reference Value	Minimum Value	Maximum Value
Salt	elastic	E_{salt}	GPa	25	20	40
		ν_{salt}	——	0.25	0.2	0.4
	viscoplastic —— L-M-S law	A	——	1	0.5	2
		α	——	0.36	0.36	0.45
		β	——	2.98	2.43	2.98
		K	MPa	0.85	0.44	0.85
Cement	elastic	E_{cem}	GPa	12	5	40
		ν_{cem}	——	0.25	0.2	0.4
	viscoplastic —— M-D law	A_1	$day^{-1} \times MPa^{-n}$	10^{-7}	0	2.10^{-7}
		n	——	1.95	1	3
		m	——	2	1	3
		α_w	——	24.42	10	30
		K_0	MPa^{-m}	$1.59 \cdot 10^{-5}$	10^{-5}	$3 \cdot 10^{-5}$
		δ	——	12	1	15

There are $k = 14$ parameters in Table 2; therefore, when each parameter is allowed to take its minimum or maximum values, there are $2^k = 16{,}384$ possible combinations in the sensibility study.

A typical example of computation results is shown in Figure 12. In this example, k = 7 varying parameters were considered; the other 7 parameters are fixed and equal to their reference value. There are 2^7=128 cases referenced at the bottom axis of the plot. For each case, the maximum value of the maximum principal stress (the less compressive stress) reached during the worst-case scenario is plotted.

In order to verify the computations, the parameter combinations providing the maximum stress on Figure 12 are considered, and a new computation is performed using a larger and more refined mesh. An example of a contour plot of the maximum principal stress, $\sigma_{\max}$, in cement around the packer at the end of blowout is shown in Figure 13 .

It appears that the most sensitive parameters are the cement elastic, salt creep and salt elastic parameters. The effect of cement viscoplasticity is relatively complex. When cement viscoplastic behavior is taken into account, stress redistribution in the cement becomes a function of time: it can reduce or increase the intensity of tensile stresses depending both on the gas-pressure history of the cavern and the parameters of the materials. The results are not sensitive to the pressure increase rate in the annular space following the onset of a gas leak.

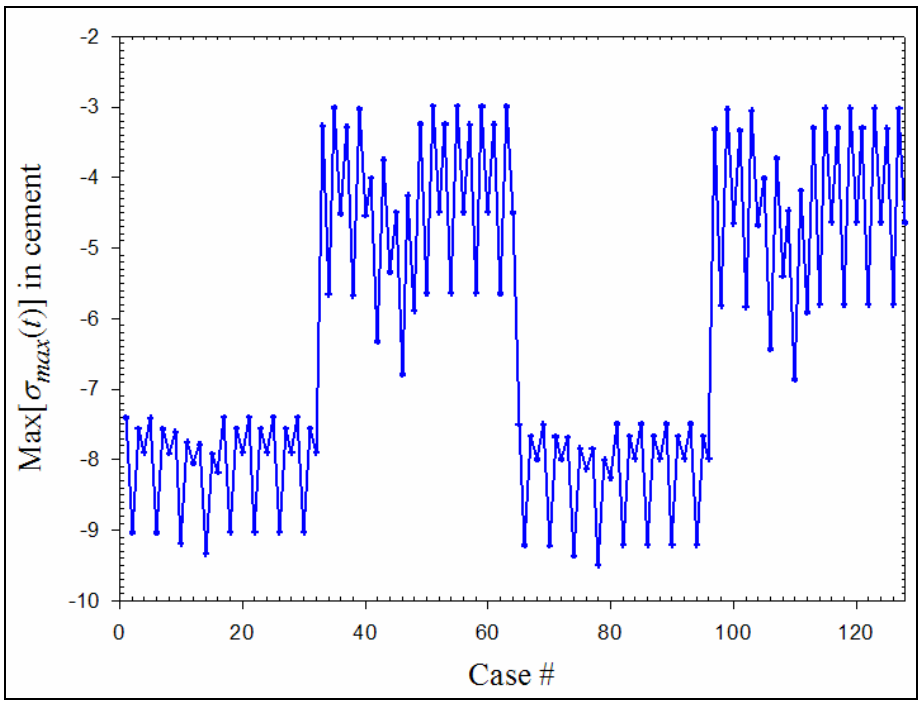

Figure 12 Example of computations results for a sensibility study of salt and cement elasto-visco-plastic parameters. (The maximum principal stress, $\sigma_{\max}$, remains positive (compressive) in the cement during the worst-case scenario.)

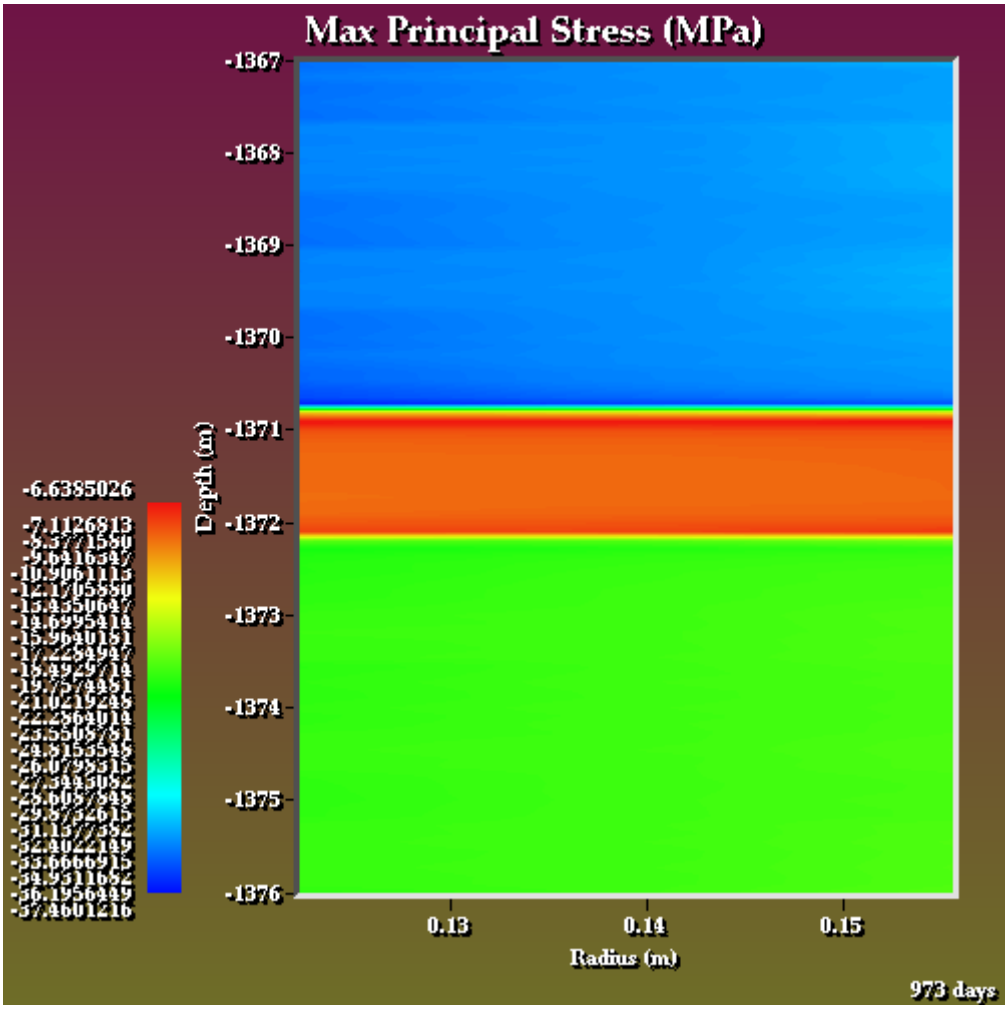

Figure 13 Maximal principal stress (σ_{max}) field in cement at the end of the blowout. (No tensile stresses appear. The less compressive stress appears at the depth of the packer — i.e., between 1371-m and 1372-m deep.)

8. Conclusions

A sensibility study comprising thousands of computations was performed to assess the influence of material mechanical parameters on the possible development of tensile stresses in cement. A finite-element toolbox was developed in the *LOCAS* software and results were compared to closed-form solutions. Finite element analyses of a worst-case scenario revealed that no damage occurs for Gaz de France studied wells, but a case-by-case study should be performed, as well geometry, especially string thickness, plays an important role.

REFERENCES

Brouard B., Karimi-Jafari M., Bérest P. and Frangi A. (2006) *Using LOCAS software to better understand the behavior of salt caverns.* Proc. SMRI Spring Meeting, Brussels, Belgium, pp. 274-288.

Munson D.E. (1997) *Constitutive model of creep in Rock salt applied to underground room closure*. Int. J. Rock Mech. Min. Sci., pp. 233-247.

Oudeman P. and Kerem M. (2004) *Transient behavior of annular pressure build-up in HP/HT wells*. 11th Abu Dhabi Int. Petroleum Exhibition and Conference, SPE paper n°88735.

Rokhar R., Staudtmeister K. and Zander-Schiebenhöfer D. (2004) *Application of a continuum damage model for cavern design case study: Atmospheric pressure*. Proc. SMRI Spring Meeting, Wichita, pp. 37-56.

Szary T., Hansen A., Rehmer P. and Brückner D. **(2004)** *Case study on consequences of cavern convergence on the integrity of cemented production casing strings based on the measurements and numerical calculations.* Proc. SMRI Fall Meeting, Berlin, Germany, pp. 331-345.